

# Assessment of Future Climate and Vegetation Canopy Change Impacts on Hydrological Behavior of Chungju Dam Watershed using SWAT Model

Min Ji Park\*, Rim Ha\*\*, Nam Won Kim\*\*\*, Kyoung Jae Lim\*\*\*\*, and Seong Joon Kim\*\*\*\*\*

Received April 4, 2012/Revised 1st: September 21, 2012, 2nd: April 19, 2013/Accepted June 12, 2013/Published Online November 30, 2013

---

## Abstract

The impact on hydrological components including evapotranspiration, soil moisture content, groundwater recharge, and dam inflow by the future potential climate and vegetation canopy changes was assessed for a dam watershed using Soil and Water Assessment Tool (SWAT) model. The SWAT model was calibrated and verified using 9 years (1997-2006) and another 7 years (1990-1996) daily dam inflow data, respectively for a 6,585.1 km<sup>2</sup> dam watershed located in the mountainous northeastern part of South Korea. The second generation coupled global climate model (CGCM2) data of Canadian Centre for Climate modelling and analysis (CCCma) from two Special Reports on Emissions Scenarios (SRES) climate change scenarios (A2 and B2) of the Intergovernmental Panel on Climate Change (IPCC) were adopted. The future vegetation canopy was developed by the nonlinear regression between monthly Leaf Area Index (LAI) from Terra MODIS (Moderate Resolution Imaging Spectroradiometer) images and monthly mean temperature of 7 years (2000-2006) data. The future prediction results with A2 and B2 scenarios showed that the maximum changes in annual dam inflow were predicted to be -18.2% in 2090s A2 scenario compared to 2000 baseline data. The future seasonal maximum dam inflow changes appeared in fall period to be -31.0% for the A2 scenario. From the contribution analysis of climate change and vegetation canopy for the overall future predicted results, the climate change primarily led the future impact on the predicted results. For the future vegetation impact on hydrological components, soil moisture was more sensitive than dam inflow and evapotranspiration.

Keywords: *climate change, MODIS, LAI, SWAT, vegetation canopy, hydrological impact, dam inflow*

---

## 1. Introduction

Global changes of climate and atmosphere CO<sub>2</sub> concentration may have direct consequences on natural resources (Chaplot, 2007). Specifically, water is one of the vital natural resources that are sensitive to climatic changes (IPCC, 1996; Gleick, 2000; Water Resources Update, 2003). Future available water resource can be evaluated by the hydrological impact studies using outputs from the General Circulation Models (GCMs). GCMs are commonly used for predicting climate change and for providing inputs to hydrological models.

Many modeling studies deal with the impact of climate change on river flows, however most of these studies are limited to the application of present vegetation cover conditions. Vegetation cover is the essential input data to hydrological models. Their changes directly affect evapotranspiration, infiltration and soil

water storage which change the dynamics of surface runoff, subsurface runoff and groundwater recharge. It is important to consider the future vegetation cover. Future vegetation cover is important for future behavior of hydrological components in addition to climate changes.

The SWAT model (Arnold *et al.*, 1998; Arnold and Fohrer, 2005) has proven to be an effective tool for assessing water resource. SWAT has gained international acceptance as a robust interdisciplinary watershed modeling tool as evidenced by international SWAT conferences, hundreds of SWAT-related papers presented at numerous other scientific meetings, and dozens of articles published in peer-reviewed journals (Gassman *et al.*, 2007). Several SWAT studies provide useful insights regarding the effects of arbitrary CO<sub>2</sub> fertilization changes and other climatic input shifts on plant growth, streamflow, and other responses (Stonefelt *et al.*, 2000, Fontaine *et al.*, 2001, and Jha *et*

---

\*Member, Environmental Researcher, Dept. of Civil and Environmental System Engineering, Konkuk University, Seoul 143-701, Korea; Water Quality Control Center, National Institute of Environmental Research, Incheon 404-708, Korea (E-mail: iamg79@korea.kr)

\*\*Member, Ph.D. Candidate, Dept. of Civil and Environmental System Engineering, Konkuk University, Seoul 143-701, Korea (E-mail: rim486@konkuk.ac.kr)

\*\*\*Member, Research Fellow, Korea Institute of Construction Technology, Ilsan 411-712, Korea (E-mail: nwkim@kict.re.kr)

\*\*\*\*Professor, Dept. of Regional Infrastructure Engineering, Kangwon National University, Gangwon-do 200-701, Korea (E-mail: kjlim@kangwon.ac.kr)

\*\*\*\*\*Member, Professor, Dept. of Civil and Environmental System Engineering, Konkuk University, Seoul 143-701, Korea (Corresponding Author, Email: kimsj@konkuk.ac.kr)

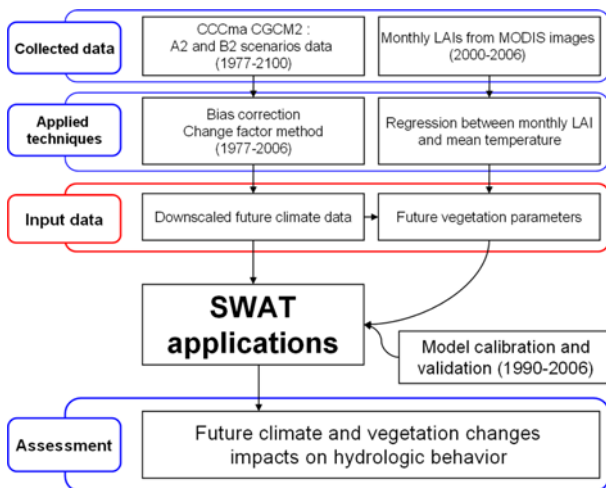


Fig. 1. The Schematic Diagram of This Study

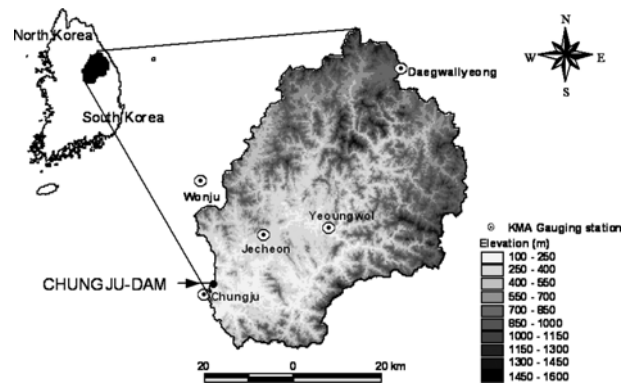


Fig. 2. The Watershed Location, Elevation and Weather Stations

*al.*, 2006). Muttiah and Wurbs (2002), Gosain *et al.* (2006) and Ryu *et al.* (2011) used SWAT to simulate the impacts of future climate change scenario on the streamflows. Rosenberg *et al.* (2003), Thomson *et al.* (2003), Rosenberg *et al.* (1999), Takle *et al.* (2005), and Jha *et al.* (2004) predicted climate change impacts on the hydrological components using GCMs, downscaling of RCM (regional climate model). Eckhardt and Ulbrich (2003) featured variable stomatal conductance and leaf area responses by incorporating different stomatal conductance decline factors and LAI values as a function of five main vegetation types.

The main goal of this study is to assess the potential impact of climate changes on hydrological components of a watershed by considering future vegetation cover conditions. The corresponding future seasonal vegetation cover conditions were derived by the MODIS LAI values estimated from the relationship of LAI-Temperature nonlinear regression. The SWAT model was applied to evaluate the future climate impact on hydrological components using the climate change results of CCCma CGCM2 based on SRES A2 and B2 for a 6,585.1 km<sup>2</sup> mountainous watershed located in the upper east part of South Korea. Fig. 1 shows the schematic diagram of this study.

## 2. Material and Method

### 2.1 Study Watershed

The study watershed, with a total area of 6,585.1 km<sup>2</sup>, is located in the northeast of South Korea within the latitude-longitude range of 127.9°E-129.0°E and 36.8°N-37.8°N (Fig. 2). The elevation ranges from 115 to 1559 m, with an average hillslope of 36.9% and an average elevation of 609 m. Chungju dam is situated at the outlet of the watershed with a height of 97.5 m, length of 447 m and storage volume of 9.7 million m<sup>3</sup>. Details for the elevation, land use, soil information, and hydrological data used in this study are found in Park *et al.* (2011).

### 2.2 SWAT (Soil & Water Assessment Tool) Model Description

SWAT (Arnold *et al.*, 1998) is a well established, distributed

eco-hydrologic model operating on a daily time step. It was developed to predict the impact of land management practices on water, sediment and agricultural chemical yields in large complex watersheds with varying soils, land use and management conditions over long periods of time. The smallest spatial subunits resolved by the model are hydrotopes (hydrologic response units), which are assumed to be homogeneous with respect to their hydrologic properties. In each hydrotope, the water balance is represented by several storage volumes: canopy storage, snow, soil profile, shallow aquifer and deep aquifer. The soil profile can be subdivided into multiple layers. Soil water processes include infiltration, evaporation, plant uptake, lateral flow and percolation to lower layers. Percolation from the bottom of the soil profile recharges the shallow aquifer. A recession constant is used to lag the flow from the aquifer to the stream. Other shallow aquifer components include evaporation, pumping withdrawals and seepage to the deep aquifer (Eckhardt *et al.*, 2005).

To predict the runoff generation, SWAT uses a modified version of the SCS (Soil Conservation Service) CN (Curve Number) method (USDA-SCS, 1972). The most important equations for runoff are presented below. The hydrologic cycle as simulated by SWAT is based on the water balance equation.

$$SW_t = SW_0 + \sum_{i=1}^t (R_{day} - Q_{surf} - E_a - w_{seep} - Q_{gw}) \quad (1)$$

where  $SW_t$  is the final soil water content (mm H<sub>2</sub>O),  $SW_0$  is the initial soil water content (mm H<sub>2</sub>O),  $t$  is the time (days),  $R_{day}$  is the amount of precipitation on day  $i$  (mm H<sub>2</sub>O),  $Q_{surf}$  is the amount of surface runoff on day  $i$  (mm H<sub>2</sub>O),  $E_a$  is the amount of evapotranspiration on day  $i$  (mm H<sub>2</sub>O),  $w_{seep}$  is the amount of percolation and bypass flow exiting the soil profile bottom on day  $i$  (mm H<sub>2</sub>O), and  $Q_{gw}$  is the amount of return flow on day  $i$  (mm H<sub>2</sub>O).

Numerous methods have been developed to estimate Potential Evapotranspiration (PET). Three of these methods have been incorporated into SWAT: the Penman-Monteith method (Monteith, 1965; Allen, 1986; Allen *et al.*, 1989), the Priestley-Taylor method (Priestley and Taylor, 1972) and the Hargreaves method (Hargreaves *et al.*, 1985). In this study, Penman-Monteith method was adopted. This equation combines components that

Table 1. Data Sets for SWAT

Data Type	Source	Scale	Data Description / Properties
Terrain	Korea National Geography Institute	1/5,000	Digital Elevation Model (DEM)
Soil	Korea Rural Development Administration	1/25,000	Soil classifications and physical properties viz. texture, porosity, field capacity, wilting point, saturated conductivity, and soil depth
Land Use	Water Management Information System	30 m	Landsat land use classification (2000 year, 9 classes)
Vegetation canopy	Terra MODIS satellite image	1 km	Leaf Area Index (LAI)
Weather	Korea Meteorological Administration	-	Daily precipitation, minimum and maximum temperature, mean wind speed and relative humidity data from 1977 to 2006
Streamflow	Han River Flood Control Office	-	Daily dam inflow data from 1987 to 2006

Table 2. Weather Stations used for SWAT Simulation

Name	Data periods	Elevation (m)	Latitude	Longitude	The average annual values	
					Precipitation (mm)	Temperature (°C)
Chungju	1977-2006	69.1	36-58-3.2	127-57-17.2	1,187.7	11.2
Daegwallyeong	1977-2006	842.5	37-41-2.9	128-45-39.6	1,717.2	6.4
Jecheon	1977-2006	263.2	37-9-23.3	128-11-46.6	1,295.0	10.1
Wonju	1977-2006	149.8	37-20-4.7	127-56-56	1,290.9	10.8
Yeungwol	1995-2006	239.8	37-10-42.6	128-27-35.6	1,326.5	10.6

account for energy needed to sustain evaporation, the strength of the mechanism required to remove the water vapor and aerodynamic and surface resistance terms. The Penman-Monteith equation is:

$$\lambda E = \frac{\Delta \cdot (H_{net} - G) + \rho_{air} \cdot c_p \cdot [e_z^0 - e_z] / r_a}{\Delta + \gamma \cdot (1 + r_c / r_a)} \quad (2)$$

where  $\lambda E$  is the latent heat flux density ( $\text{MJ}/\text{m}^2 \cdot \text{d}$ ),  $\Delta$  is the depth rate evaporation ( $\text{mm}/\text{d}$ ), is the slope of the saturation vapor pressure-temperature curve,  $de/dT$  ( $\text{kPa}/^\circ\text{C}$ ),  $H_{net}$  is the net radiation ( $\text{MJ}/\text{m}^2 \cdot \text{d}$ ), is the heat flux density to the ground ( $\text{MJ}/\text{m}^2 \cdot \text{d}$ ),  $\rho_{air}$  is the air density ( $\text{kg}/\text{m}^3$ ),  $c_p$  is the specific heat at constant pressure ( $\text{MJ}/\text{kg} \cdot ^\circ\text{C}$ ),  $e_z^0$  is the saturation vapor pressure of air at height  $z$  ( $\text{kPa}$ ),  $e_z$  is the water vapor pressure of air at height  $z$  ( $\text{kPa}$ ),  $\gamma$  is the psychrometric constant ( $\text{kPa}/^\circ\text{C}$ ),  $r_c$  is the plant canopy resistance ( $\text{s}/\text{m}$ ), and  $r_a$  is the diffusion resistance of the air layer (aerodynamic resistance) ( $\text{s}/\text{m}$ ).

Plant canopy resistance is estimated by dividing the minimum surface resistance for a single leaf by one-half of the canopy LAI (Jensen *et al.*, 1990):

$$r_c = r_l / (0.5 \cdot LAI) \quad (3)$$

where  $r_c$  is the canopy resistance ( $\text{s}/\text{m}$ ),  $r_l$  is the minimum effective stomatal resistance of a single leaf ( $\text{s}/\text{m}$ ), and  $LAI$  is the leaf area index of the canopy.

### 2.3 The Spatial, Weather and Dam Inflow Data

The SWAT model requires data on elevation, land use, soil and weather to assess the water yield at the desired locations of the watershed. Elevation data were rasterized from a vector map of 1:5,000 scale that was supplied by the Korea National Geography Institute. Based on the Digital Elevation Model, the watershed was divided into 18 sub-basins. Soil data were rasterized from a vector map of 1:50,000 scale that was supplied by the Korea

Rural Development Administration. The 2000 Landsat land use data were obtained from the Water Management Information System (<http://www.wamis.go.kr/eng/main.aspx>) operated by Ministry of Land, Infrastructure and Transport. The monthly MODIS Leaf Area Index was prepared for Penman-Monteith evapotranspiration (ET). The dam inflow has been gauged since 1974 by the Korea Water Resources Corporation (K-water) (Table 1).

Five weather stations closest to the watershed were selected as seen in Fig. 2 and Table 2 summarizes the characteristics of weather stations. The 30 years (1977-2006) daily maximum; and minimum air temperatures ( $^\circ\text{C}$ ), daily precipitation ( $\text{mm}$ ), relative humidity ( $\%$ ), wind speed ( $\text{m}/\text{sec}$ ), and solar radiation ( $\text{MJ}/\text{m}^2$ ) were obtained from the Korea Meteorological Administration (KMA).

### 2.4 The Future Climate Data

For future climate data, the CCCma CGCM2 data by two SRES climate change scenarios (A2 and B2) of the IPCC were adopted. The atmospheric component of the model is a spectral model with triangular truncation at wave number 32 yielding a surface grid resolution of roughly  $3.7^\circ$  by  $3.7^\circ$  and 10 vertical levels (IPCC, 2006). Here, A2 is “high” GHG emission scenario and B2 is “low” GHG emission scenario respectively.

In this study, a downscaling was performed by two steps. Firstly, the GCM data was corrected to ensure that 30 years observed data (1977-2006, baseline period) and GCM model output of the same period have similar statistical properties by the method used by Alcamo *et al.* (1997) and Droogers and Aerts (2005) among the various statistical transformations. Details for this method the results are found in Park *et al.* (2011).

Secondly, GCM model was downscaled using Change Factor (CF) method (Diaz-nieto and Wilby, 2005; Wilby and Harris,

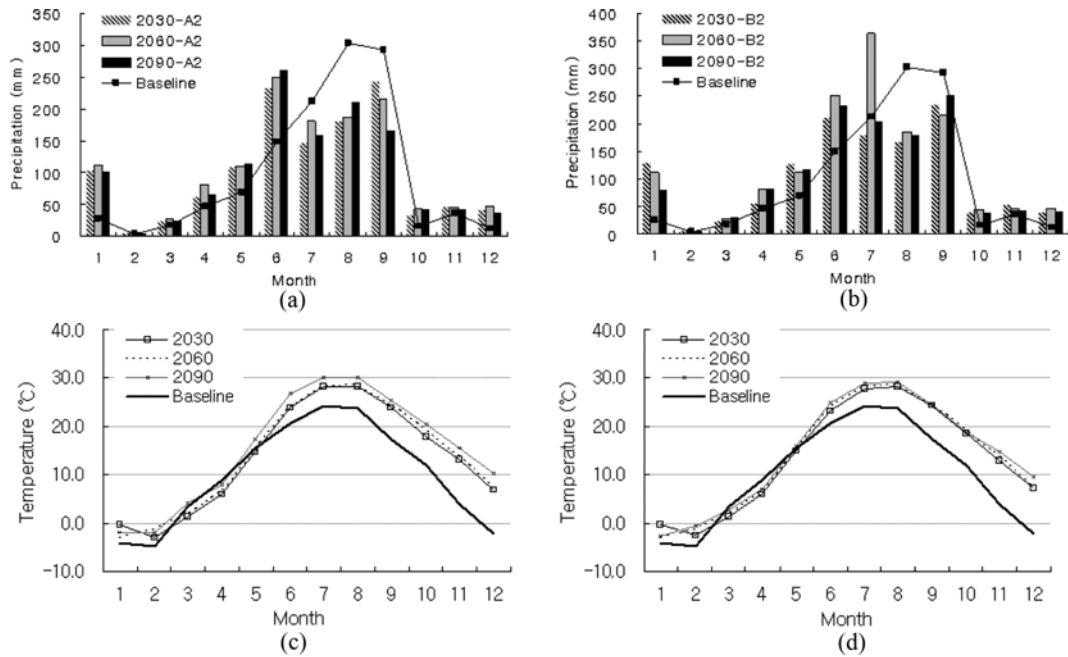


Fig. 3. The Future Adjusted and Downscaled Temperature and Precipitation Scenarios by CF Downscaling Method after Correcting the GCM Data by 30-year Historical Data: (a) Precipitation (A2), (b) Precipitation (B2), (c) Temperature (A2), (d) Temperature (B2)

Table 3. The Changes (In Millimeter) in Seasonal Precipitation for the CF Method

Scenario	2030s		2060s		2090s	
	A2	B2	A2	B2	A2	B2
Winter (December-February)	+107.7	+132.7	+119.7	+119.7	+101.9	+84.6
Spring (March-May)	+61.8	+73.6	+86.9	+86.9	+70.3	+96.8
Summer (June-August)	-102.5	-107.9	-47.2	+135.2	-34.1	-46.6
Fall (September-November)	-21.5	-14.8	-40.1	-40.1	-92.6	-10.1
Total	+45.5	+83.5	+119.4	+301.8	+45.5	+124.7

Table 4. The Changes (In Degree) in Seasonal Temperature for the CF Method

Scenario	2030s		2060s		2090s	
	A2	B2	A2	B2	A2	B2
Winter (December-February)	+4.8	+5.2	+4.7	+4.7	+5.8	+5.8
Spring (March-May)	-1.9	-1.9	-1.4	-1.4	+0.5	-0.6
Summer (June-August)	+3.8	+3.5	+4.0	+4.0	+6.1	+4.8
Fall (September-November)	+7.3	+7.6	+8.2	+8.2	+9.5	+8.3
Average	+3.5	+3.6	+3.9	+3.9	+5.5	+4.6

2006). Ahn *et al.* (2011) has a detailed description about this process. The results are found in Fig. 3 for the future monthly temperature and precipitation scenarios respectively. The results showed that there are 5.5°C temperature and 45.5 mm precipitation increase in case of A2 scenario, and 4.6°C temperature and 124.7 mm precipitation increase in case of B2 scenario for 2090 (Tables 3 and 4).

### 2.5 The Future Vegetation Data

To predict the future vegetation cover information, a nonlinear regression between monthly LAI of each land cover from MODIS satellite image and monthly mean temperature was accomplished.

The MODIS LAI 8-days composite scenes (MODIS A2, Collection 3) from 2000 to 2006 were downloaded from the Earth Observing System Data Gateway (<http://edcimswww.cr.usgs.gov/pub/imswelcome/index.html>), especially V003 (known as collection 3 provisional data). Fig. 4 shows the monthly MODIS LAI of each land cover from 2000 to 2006. Details for LAI the results are found in Ha *et al.* (2010).

Table 5 and Fig. 5 show the nonlinear regression result using seven years (2000-2006) monthly LAI and monthly mean temperature from March to November. The monthly LAIs of each land use from December to February could not be derived because of snow cover, thus they were extrapolated using the

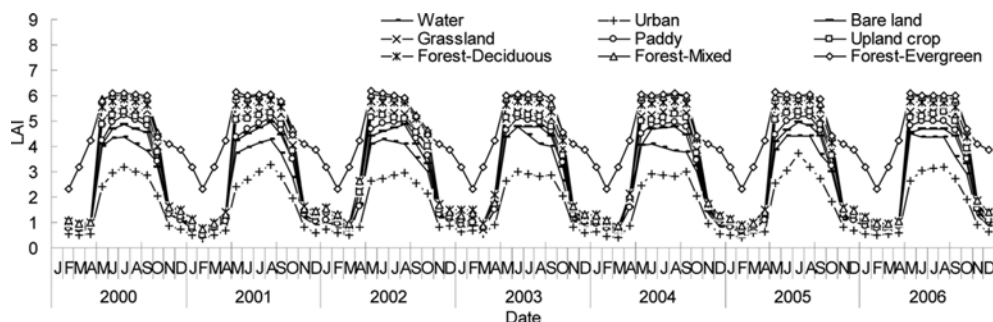


Fig. 4. The Monthly MODIS LAI of Each Land Cover from 2000 to 2006

Table 5. The Derived Nonlinear Regression Equation between Monthly Mean Temperature and MODIS Monthly LAI for Each Land use Class

Land use class	Regression equation	R <sup>2</sup>
Grassland	$LAI = \frac{1.056 - 5.425}{1 + e^{(Temp - 11.382)/2.042}} + 5.425$	0.93
Paddy	$LAI = \frac{0.933 - 5.071}{1 + e^{(Temp - 12.081)/2.326}} + 5.071$	0.93
Upland crop	$LAI = \frac{1.063 - 5.244}{1 + e^{(Temp - 11.471)/2.023}} + 5.244$	0.93
Forest-Deciduous	$LAI = \frac{1.167 - 5.8}{1 + e^{(Temp - 11.211)/1.990}} + 5.8$	0.92
Forest-Mixed	$LAI = \frac{1.224 - 6.06}{1 + e^{(Temp - 11.632)/1.742}} + 6.06$	0.93
Forest-Evergreen	$LAI = \frac{3.19 - 6.18}{1 + e^{(Temp - 11.551)/2.640}} + 6.18$	0.90

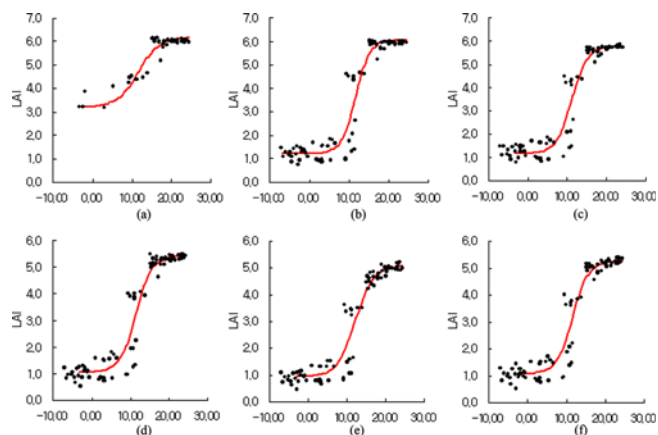


Fig. 5. The Derived Nonlinear Regression Equation between Temperature and MODIS Monthly LAI for Each Land use Class: (a) Forest-Evergreen, (b) Forest-Mixed, (c) Forest-Deciduous, (d) Grassland, (e) Paddy, (f) Upland Crop

nonlinear regression. The future LAIs for each land uses were estimated using the future downscaled temperatures. SWAT uses 6 parameters about LAI as shown in Table 6. FRGRW and DLAI

are related to the growth period of each land use, and LAIMX and BLAI are the LAI corresponding to the period. We calculated future monthly LAI with the future monthly temperature, and extracted the growth period and LAI from the parameters using the monthly LAI. Table 6 shows the future A2 and B2 predicted

Table 6. The Future Predicted Vegetation Parameters of Forest Land use for A2 and B2 Scenarios of GCM

	FRGRW1 <sup>d</sup>			LAIMX1 <sup>e</sup>			FRGRW2 <sup>d</sup>			LAIMX2 <sup>e</sup>			BLAI <sup>f</sup>			DLAI <sup>g</sup>			
	E <sup>a</sup>	M <sup>b</sup>	D <sup>c</sup>	E <sup>a</sup>	M <sup>b</sup>	D <sup>c</sup>	E <sup>a</sup>	M <sup>b</sup>	D <sup>c</sup>	E <sup>a</sup>	M <sup>b</sup>	D <sup>c</sup>	E <sup>a</sup>	M <sup>b</sup>	D <sup>c</sup>	E <sup>a</sup>	M <sup>b</sup>	D <sup>c</sup>	
Present	0.15	0.05	0.05	0.70	0.05	0.05	0.25	0.4	0.4	0.99	0.95	0.95	5.00	5.00	5.00	0.99	0.99	0.99	
A2 scenario																			
2030s	0.25	0.10	0.10	0.55	0.22	0.23	0.42	0.27	0.27	0.98	0.82	0.82	6.18	6.06	5.80	0.92	0.82	0.82	
2060s	0.25	0.10	0.10	0.56	0.22	0.24	0.42	0.27	0.27	0.99	0.82	0.82	6.18	6.06	5.80	0.92	0.82	0.82	
2090s	0.25	0.10	0.10	0.56	0.23	0.22	0.42	0.27	0.27	0.99	0.82	0.82	6.18	6.06	5.80	0.92	0.82	0.82	
B2 scenario																			
2030s	0.25	0.10	0.10	0.55	0.22	0.24	0.42	0.27	0.27	0.98	0.82	0.82	6.18	6.06	5.80	0.92	0.82	0.82	
2060s	0.25	0.10	0.10	0.55	0.22	0.24	0.42	0.27	0.27	0.98	0.82	0.82	6.18	6.06	5.80	0.92	0.82	0.82	
2090s	0.25	0.10	0.10	0.56	0.22	0.24	0.42	0.27	0.27	0.99	0.82	0.82	6.18	6.06	5.80	0.92	0.82	0.82	

<sup>a</sup>Forest-Evergreen

<sup>b</sup>Forest-Mixed

<sup>c</sup>Forest-Deciduous

<sup>d</sup>Fraction of the growing season corresponding to the 1<sup>st</sup> and 2<sup>nd</sup> point on the optimal leaf area development curve respectively

<sup>e</sup>Fraction of the maximum plant leaf area index corresponding to the 1<sup>st</sup>, 2<sup>nd</sup> point on the optimal leaf area development curve respectively

<sup>f</sup>Potential maximum leaf area index for the plant

<sup>g</sup>Fraction of growing season at which senescence becomes the dominant growth process

vegetation parameters of forest land uses.

### 3. Results and Discussion

#### 3.1 SWAT Calibration and Validation

Based on the DEM, the watershed was divided into 25 subbasins. The SWAT model was calibrated for 10 years (1997-2006) daily streamflow records and validated for another 7 years (1990-1996). The calibration of streamflow was performed in two steps. First, the long-term balance was calibrated to match the total flow, peak flow and base flow by minimizing the difference in average annual flows. Second, the daily observed and simulated flow data was calibrated by Nash and Sutcliffe Model Efficiency (ME) (Nash and Sutcliffe, 1970), coefficients of determination ( $R^2$ ) and Root Mean Square Error (RMSE).

Table 7 shows the calibrated parameters comparing with the values of other four studies. Fig. 6 and Fig. 7 show the observed versus simulated dam inflow for calibration and validation periods, respectively and a statistical summary is shown in Table 8. The simulated runoff ratio was somewhat overestimated for the calibration and validation periods. The ME ranged from 0.43 to 0.91, the coefficients of determination ranged from 0.59 to 0.92, and the root mean square error ranged from 1.0 to 2.9 mm. Then the values for ME and  $R^2$  are equal to one, the model prediction is considered to be perfect. The ME values imply that the model predicted from 43% to 91% better than using the average dam inflow value during the study period.

#### 3.2 Hydrologic Impacts by Future Climate Change Considering Vegetation Canopy Change

For the evaluation of climate and vegetation canopy change impact on dam inflow, the SWAT model was run with the future downscaled climate data and the future predicted MODIS LAI

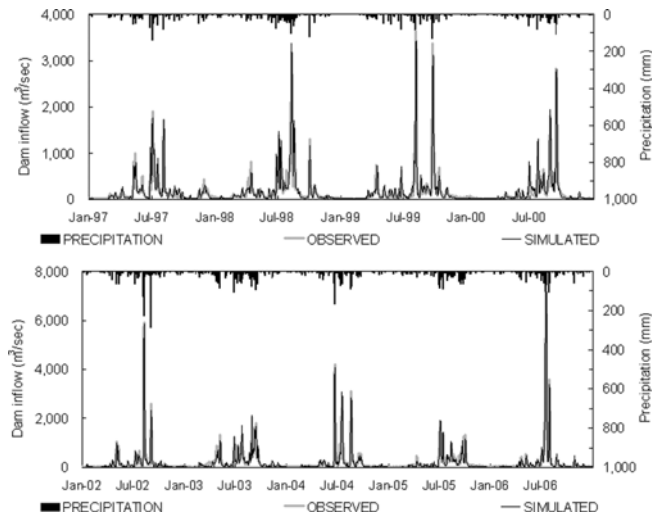


Fig. 6. Calibration Results (1997-2006)

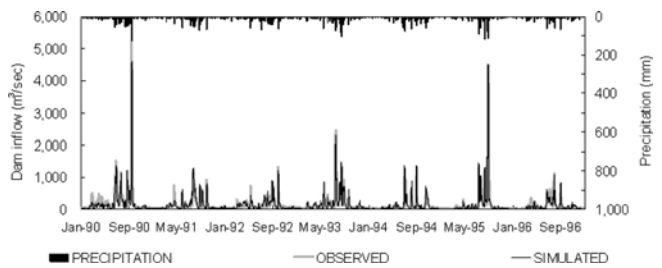


Fig. 7. Validation Results (1990-1996)

vegetation information. A key for long-term planning and management of water resources considering future changes in the pattern of climate, water demand and water availability in a watershed is not only the possible changes to annual hydrologic components under climate changes but also how seasonal

Table 7. The Calibrated Parameters for the SWAT Model

Parameter name	Description	Range	This study	Zhang (2007)	Heuvelmans et al. (2006)	Muleta and Nicklow (2005)	Bärlund et al. (2007)
CN2	Curve number adjustment ratio	0 ~ 10	-8	-4 ~ +2	(forest) 55	-	-16 ~ +24
CH_K2	Effective hydraulic conductivity in main channel alluvium (mm/hr)	0 ~ 50	50	-	-	-	-
ESCO	Soil evaporation compensation	0 ~ 1	0.2	0.4	-	0.0882	-
EPCO	Plant uptake compensation factor	0 ~ 1	0.2	0.2	-	1	-
ALPHA_BF	Base flow recession constant	0 ~ 1	0.2	0.43	0.5	-	0.15~0.46
SMFMX	Maximum snowmelt factor	0 ~ 10	6	8.3	-0.2	-	-
SMFMN	Minimum snowmelt factor	0 ~ 10	2	5.5	-0.1	-	-
TIMP	Snow pack temperature lag factor	0 ~ 1	0.5	-	0.5	-	-
SNOCOVMX	Threshold depth of snow, above which there is 100% cover	0 ~ 500	50	-	10	-	-
SNO50COV	Fraction of snow volume represented by SNOCOVMX that corresponds to 50% snow cover	0 ~ 1	0.5	-	-	-	-
GW_REVAP	Coefficient controlling water movement between root zone and shallow aquifer	0.02 ~ 0.2	0.2	-	-	-	0.10 ~0.18
REVAPMN	Threshold depth of water in the shallow aquifer for 're-evap' to occur (mm)	0 ~ 500	400	-	-	28.2478	0 ~45

Table 8. Summary of Model Calibration and Verification

Year	Observed			Simulated			Statistical summary			Note <sup>h</sup>
	P (mm) <sup>a</sup>	Q (mm) <sup>b</sup>	QR (%) <sup>c</sup>	Q (mm) <sup>b</sup>	QR (%) <sup>b</sup>	ET (mm) <sup>d</sup>	RMSE (mm/day) <sup>e</sup>	R <sup>2f</sup>	ME <sup>g</sup>	
1990	1837.8	1038.2	56.5	974.0	53.0	531.2	2.1	0.88	0.88	V
1991	1447.7	527.6	36.4	639.8	44.2	481.5	1.2	0.77	0.70	V
1992	1281.8	506.8	39.5	576.8	45.0	481.7	1.1	0.69	0.64	V
1993	1538.1	751.7	48.9	788.5	51.2	470.2	1.6	0.83	0.82	V
1994	1208.6	381.5	31.6	442.6	36.6	392.7	1.4	0.59	0.43	V
1995	1262.9	661.4	52.4	774.2	61.3	433.7	2.2	0.87	0.83	V
1996	1042.5	384.7	36.9	448.2	43.0	432.5	1.0	0.71	0.58	V
Average	1374.2	607.4	43.2	663.4	47.8	460.5	1.5	0.76	0.76	-
1997	1394.4	631.2	45.3	751.5	53.9	500.6	1.7	0.78	0.67	C
1998	1778.2	856.3	48.1	948.2	53.3	538.8	1.7	0.89	0.86	C
1999	1595.1	792.4	49.7	881.3	55.2	515.5	2.1	0.87	0.86	C
2000	1187.0	587.1	49.4	718.6	61.4	410.7	1.6	0.87	0.83	C
2001	919.8	296.6	32.2	346.1	37.6	410.7	1.1	0.70	0.45	C
2002	1718.6	821.8	47.8	895.9	52.1	516.8	2.2	0.91	0.91	C
2003	1856.7	1018.4	54.8	1086.7	58.5	560.1	1.7	0.84	0.85	C
2004	1503.8	892.3	59.3	958.5	63.7	528.2	2.4	0.88	0.86	C
2005	1469.6	726.9	49.5	802.9	54.6	522.7	1.4	0.86	0.84	C
2006	1613.7	936.3	58.0	1093.3	67.7	493.5	2.9	0.92	0.90	C
Average	1568.6	807.0	51.3	904.1	57.8	509.7	2.0	0.87	0.84	-

<sup>a</sup>Precipitation

<sup>b</sup>Dam inflow

<sup>c</sup>Runoff ratio (Q/P)

<sup>d</sup>Evapotranspiration

<sup>e</sup>Root mean square error

<sup>f</sup>Coefficient of determination

<sup>g</sup>Nash and Sutcliffe model efficiency

<sup>h</sup>V: validation; C: calibration

hydrologic components may change. Fig. 8 shows the predicted dam inflow, watershed average Penman-Monteith evapotranspiration and soil moisture content of 2030s, 2060s and 2090s for A2 and B2 scenarios. Fig. 9 shows the monthly changes in dam inflow, evapotranspiration and soil moisture content respectively with 2000 as the base year. Table 9 summarizes the future predicted annual and seasonal hydrologic components.

For the 2030s, 2060s, and 2090s A2 scenario, the annual dam inflows were predicted to change -17.6%, -16.8%, and -18.2%, respectively, and for the B2 scenario, they were predicted to change -16.0%, -12.9%, and -14.2% respectively. As time passes, the decreasing gaps in annual dam inflow between A2 and B2 scenarios increased by 1.6%, 3.9%, and 4.0%, respectively (Table 9). As shown by the seasonal changes in Table 9, the future maximum possible dam inflow changes in winter, spring, summer, and fall period were within +369%, +66%, -26%, and -48% for A2 scenario and +473%, +74%, ±25%, and -33% for B2 scenario respectively. These prediction results directly come from the future predicted precipitation and temperature as shown in Fig. 3 and Tables 3 and 4. The increased future winter snowfall and temperature will increase the dam inflow through enhanced snowmelt. Meanwhile, the future increased spring rainfall (within +100 mm per 3 months) and decreased temperature (within ± 2°C) compensated the dam inflow change by ± 3%.

Especially, the future dam inflow in fall period showed considerable changes by the decreased rainfall and the highest increase in future temperature among the seasons. The overall future possible dam inflow increased in 4 months (January, April, May, and June) and decreased in other 8 months for all scenarios as shown in Fig. 8. Thus, we can infer that the future management of reservoir water levels should be more conservative in winter and spring periods, and the future dam operation such as water supply and release principles during summer and fall periods has to be carried out more carefully than the present situation even with a restricted water supply plan and a high risk management for flood control.

In A2 and B2 scenarios of 2030s, the future possible evapotranspiration changes in spring, summer and fall were within +39% compared to 2000 baseline data. The maximum evapotranspiration change in winter showed the reaching to +142.7% and +146.9% respectively (Table 9). Especially, the future January evapotranspiration showed a considerable change by the future decrease of forest-evergreen area and the highest increase in future snowfall among the months. The future evapotranspiration change increased in all months except April and October (Fig. 9b).

According to the future increase of ET, the future soil moisture decreased in all seasons. Especially, the 2030s A2 and B2 soil

Table 9. Summary of the Future Predicted Annual and Seasonal Hydrologic Components

Period	P (mm) <sup>a</sup>	Q (mm) <sup>b</sup>	QR (%) <sup>c</sup>	Q variation (%)	ET (mm) <sup>d</sup>	ETR (%) <sup>e</sup>	ET variation (%)	SW (%) <sup>f</sup>	SW difference (%)
2000 [Baseline]									
Winter <sup>g</sup>	43.3	13.1	30.4	-	21.7	50.0	-	19.4	-
Spring <sup>h</sup>	132.4	61.6	46.5	-	112.4	84.9	-	12.3	-
Summer <sup>i</sup>	664.5	403.2	60.7	-	202.8	30.5	-	24.7	-
Fall <sup>j</sup>	343.9	247.4	71.9	-	118.1	34.3	-	20.6	-
Annual	1187.0	725.4	61.4	-	462.9	39.0	-	19.2	-
A2 scenario – 2030s									
Winter <sup>g</sup>	151.0	61.4	40.7	367.4	52.1	34.5	140.5	15.1	-4.3
Spring <sup>h</sup>	194.2	86.3	44.4	40.1	133.9	69.0	19.2	10.5	-1.8
Summer <sup>i</sup>	562.0	296.6	52.8	-26.4	256.6	45.7	26.5	12.2	-12.5
Fall <sup>j</sup>	322.4	181.8	56.4	-26.5	142.6	44.2	20.8	10.6	-9.9
Annual	1229.5	626.1	50.9	-2.8	585.3	47.6	28.7	12.1	-7.1
A2 scenario – 2060s									
Winter <sup>g</sup>	163.0	61.6	37.8	368.6	52.6	32.3	142.7	16.9	0.7
Spring <sup>h</sup>	219.3	102.2	46.6	65.9	153.3	69.9	36.4	13.0	-12.5
Summer <sup>i</sup>	617.3	334.4	54.2	-17.1	273.5	44.3	34.8	12.2	-9.8
Fall <sup>j</sup>	303.7	166.5	54.8	-32.7	143.5	47.2	21.5	10.7	-2.5
Annual	1303.4	664.7	51.0	-2.6	622.8	47.8	36.9	13.2	-6.0
A2 scenario – 2090s									
Winter <sup>g</sup>	145.1	52.8	36.4	301.5	49.7	34.3	129.5	15.2	-12.2
Spring <sup>h</sup>	202.7	92.5	45.6	50.2	139.9	69.0	24.5	10.9	-10.3
Summer <sup>i</sup>	630.4	343.7	54.5	-14.8	273.2	43.3	34.7	12.6	-4.2
Fall <sup>j</sup>	251.2	127.8	50.9	-48.3	133.4	53.1	13.0	10.2	-2.0
Annual	1229.5	616.7	50.2	-4.2	596.1	48.5	31.0	12.2	-7.0
B2 scenario – 2030s									
Winter <sup>g</sup>	176.0	75.3	42.8	472.7	53.5	30.4	146.9	17.3	-2.0
Spring <sup>h</sup>	206.0	95.9	46.6	55.8	142.7	69.3	27.0	13.2	1.0
Summer <sup>i</sup>	556.6	303.7	54.6	-24.7	249.7	44.9	23.1	13.1	-11.6
Fall <sup>j</sup>	329.0	183.5	55.8	-25.8	144.9	44.1	22.8	11.2	-9.4
Annual	1267.5	658.3	51.9	-0.8	590.8	46.6	29.9	13.7	-5.5
B2 scenario – 2060s									
Winter <sup>g</sup>	163.0	62.0	38.0	371.8	52.6	32.3	143.0	16.9	-2.4
Spring <sup>h</sup>	219.3	102.8	46.9	67.0	153.3	69.9	36.4	13.0	0.8
Summer <sup>i</sup>	799.7	461.1	57.7	14.4	275.4	34.4	35.8	11.6	-13.2
Fall <sup>j</sup>	303.7	167.1	55.0	-32.5	143.9	47.4	21.9	10.3	-10.2
Annual	1485.8	793.0	53.4	1.9	625.2	42.1	37.4	13.0	-6.3
B2 scenario – 2090s									
Winter <sup>g</sup>	127.9	44.4	34.7	237.6	50.3	39.3	132.1	14.3	-5.1
Spring <sup>h</sup>	229.2	107.1	46.7	74.0	147.0	64.1	30.8	10.5	-1.7
Summer <sup>i</sup>	617.9	345.2	55.9	-14.4	265.0	42.9	30.6	7.0	-17.8
Fall <sup>j</sup>	333.8	191.2	57.3	-22.7	146.7	44.0	24.3	8.3	-12.3
Annual	1308.7	687.9	52.6	0.4	609.0	46.5	33.9	10.0	-9.2

<sup>a</sup>Precipitation

<sup>b</sup>Dam inflow

<sup>c</sup>Runoff ratio (Q/P)

<sup>d</sup>Evapotranspiration

<sup>e</sup>ETR=ET/P\*100

<sup>f</sup>Soil moisture content

<sup>g</sup>December-February

<sup>h</sup>March-May

<sup>i</sup>June-August

<sup>j</sup>September-November



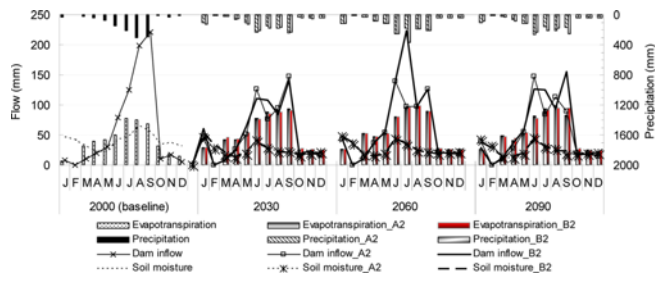


Fig. 8. The Predicted Dam Inflow, Watershed Average Penman-Monteith Evapotranspiration and Soil Moisture Content of 2030s, 2060s and 2090s for A2 and B2 Scenarios

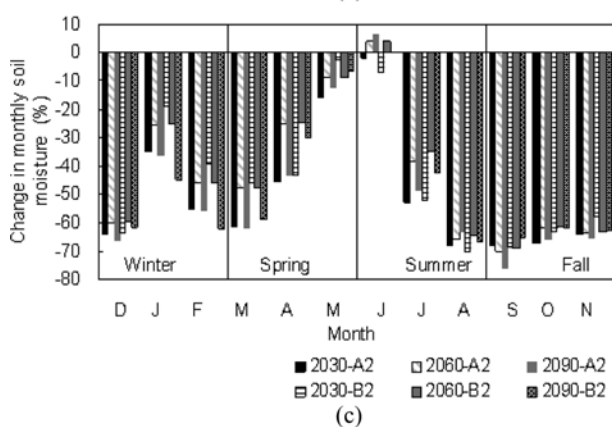
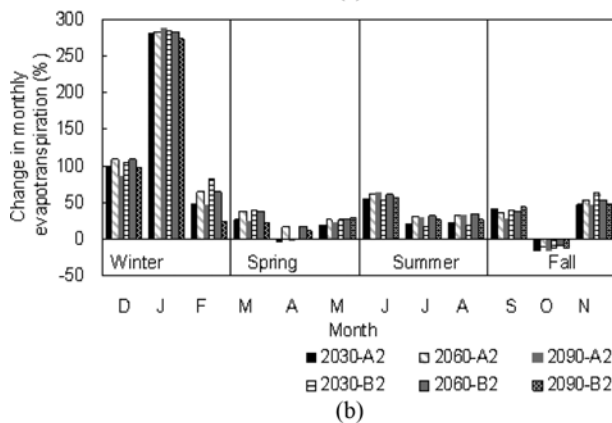
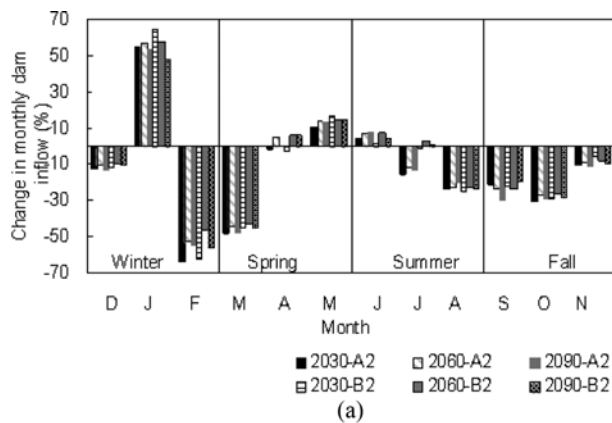


Fig. 9. The Percentage of Monthly Changes in: (a) Dam Inflow, (b) Evapotranspiration, (c) Soil Moisture Content of 2030s, 2060s and 2090s with 2000 Baseline

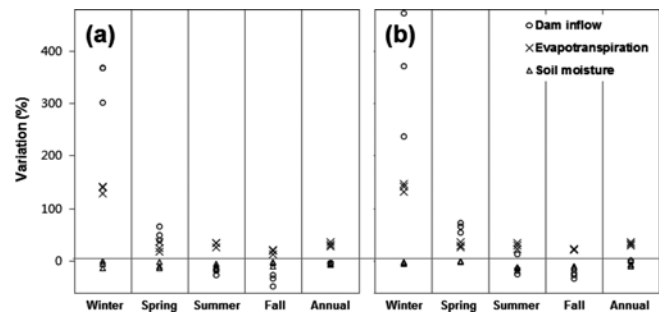


Fig. 10 Variations of Dam Inflow, Evapotranspiration and Soil Moisture Content for A2 and B2 Scenarios

moisture showed the highest changes of -13.7% and -13.2% in fall period respectively. The future soil moisture changes in other seasons were predicted to be within -12%. Thus we can infer that the big decrease of future soil moisture in fall period by the future rainfall decrease and ET increase would cause fall drought which affects the crop growth and yield negatively, and the decrease of baseflow to the stream.

For 2090s A2 and B2 scenarios, the future evapotranspiration and soil moisture changes showed a similar trend like 2030s scenarios as shown in Fig. 10. The 2090s ET changes in annual base were +1.5% and 1.8% deeper than the 2030s ET changes for A2 and B2 scenarios, respectively.

### 3.3 Contribution Analysis of Climate Factors to Future Predicted Results

A multiple regression analysis was conducted to understand which climate factors affected the future predicted results of dam inflow, evapotranspiration, and soil moisture content, respectively. Table 10 summarizes the results of multiple regression analysis between climate factors and hydrological components. The analysis showed that the future dam inflow showed significance with precipitation. The future soil moisture and evapotranspiration were significant for both precipitation and temperature. The p-values are consistently below 0.0001 and the R<sup>2</sup> values are greater than 0.8 for dam inflow and evapotranspiration. Soil moisture and temperature were only in inverse proportion to each other.

The standardized coefficients in Table 10 show that evapotranspiration was more affected by temperature (R<sup>2</sup> = 0.556) than precipitation (R<sup>2</sup> = 0.426) while dam inflow and soil moisture were greatly affected by precipitation. The regression results reflect that evapotranspiration increased and soil moisture decreased independent of the variation in precipitation under most scenarios, and most seasonal dam inflow changed by precipitation as shown in Table 9. Thus, the future control of evapotranspiration, for example, reforestation and/or forest thinning plans are necessary for securing of our future water resources availability in a mountainous watershed.

### 3.4 Contribution Analysis of Future Climate and Vegetation Canopy Changes for the Predicted Results

To identify how much the future climate change and vegetation

Table 10. Summary of Multiple Regression Analysis: Climate Factors vs. Hydrologic Components

Components	Constant	Unstandardized coefficients		Standardized coefficients		R <sup>2</sup>	P-value
		Precipitation	Temperature	Precipitation	Temperature		
Dam inflow	-9.151	0.613	-	0.989	-	0.98	0.000
Evapotranspiration	12.145	0.150	1.598	0.426	0.556	0.87	0.000
Soil moisture	8.573	0.063	-0.307	0.985	-0.591	0.39	0.000

Table 11. The Contribution Ratio of Climate Change and Vegetation Canopy for the Total Future Predicted Results

Contribution components	Scenario	A2			B2			
		Year	Dam inflow (%)	Evapotranspiration (%)	Soil moisture (%)	Dam inflow (%)	Evapotranspiration (%)	Soil moisture (%)
Vegetation canopy	2030s		0.1	0.5	8.4	0.1	0.5	8.4
	2060s		0.4	0.6	8.6	0.0	0.5	8.5
	2090s		0.4	0.6	8.4	0.0	0.5	8.6
Climate change	2030s		6.3	28.1	31.6	6.2	29.4	26.8
	2060s		0.5	36.3	25.1	1.1	36.9	24.5
	2090s		6.7	30.5	30.9	1.9	33.3	29.2

canopy change contributed to the future predicted results, the model was run with the future climate change scenarios while the vegetation canopy is kept up with the present condition. Table 11 summarizes the contribution results of climate change and vegetation canopy for the total future predicted results. Among the total future impacts, the vegetation canopy change affected at the maximum of 0.4%, 0.6%, and 8.6% for dam inflow, evapotranspiration, and soil moisture, respectively. Soil moisture was only affected up to 8.6% from the vegetation canopy. Plant management, therefore, should be considered to take measures against water depletion due to climate change.

The climate change mostly led the future impact on the predicted results. The climate change affected at the maximum of 6.7%, 36.9%, and 31.6% for dam inflow, evapotranspiration, and soil moisture, respectively.

#### 4. Conclusions

In this study, the hydrological model SWAT was applied to assess the potential impact of climate change on dam inflow by considering future vegetation cover conditions. A 6,585.1 km<sup>2</sup> mountainous dam watershed located in the middle-eastern part of South Korea, which has 84.4% forest and 10.9% paddy land uses was selected. Before the future climate change assessment, the SWAT model was calibrated and validated by comparing daily observed with simulated dam inflow results for 16 years (1990-2006) excluding 2001. The average Nash-Sutcliffe model efficiency for 7 years model validation (1990-1996) was 0.76.

For future climate condition, the CCCma CGCM2 data based on SRES A2 and B2 were adopted. The future weather data was corrected by the past weather data (1977-2006) and downscaled by the CF method. The 2090s A2 and B2 downscaled data showed +5.5°C and +4.6°C temperature increase, and 25.6 mm and 63.1 mm precipitation increase respectively. To predict the future vegetation cover information, a nonlinear regression

between monthly LAI of each land cover from MODIS satellite image and monthly mean temperature was accomplished using seven years (2000-2006) data. The 2090 future maximum LAIs for deciduous, mixed and evergreen forests increased 0.80, 1.06, and 1.18 compared to 2000 MODIS LAI values, respectively.

For the future A2 and B2 scenarios, the maximum changes in annual dam inflow were -18.2% in 2090s and -17.6% in 2030s. As time passes, the decrease gaps in annual dam inflow between A2 and B2 scenarios increased from +1.6% to +4.0%. The future seasonal maximum dam inflow changes appeared in fall period and predicted to be -30% for A2 scenario and -25% for B2 scenario. The reason was from the considerable decrease in rainfall and the highest increase in future temperature among the seasons. From the results, the future dam operation such as water supply and flood control release principles during fall periods has to be carried out more carefully than the present situation.

The maximum possible A2 and B2 evapotranspiration changes were appeared in 2060s winter period reaching to +164.1% and +164.5% compared to 2000 baseline data while other periods were within +31%. Especially, the future January evapotranspiration showed a considerable change by the future decrease of forest-evergreen area and the highest increase in future snowfall among the months. According to the future increase of ET, the future soil moisture decreased in all seasons. The maximum A2 and B2 soil moisture changes were appeared in 2090s and 2060s fall periods showing -13.6% and -13.5% respectively. The large decrease of future soil moisture in fall period would affect the crop growths and their yields negatively. Furthermore, as described in the dam inflow impact, the decreased groundwater recharge would decrease the baseflow, finally resulting in the decrease in dam inflow.

From the contribution analysis of climate factors to future predicted results, the future soil moisture and evapotranspiration were dependent on both precipitation and temperature, and the future dam inflow was dominated by precipitation. From the

contribution analysis of climate change and vegetation canopy for the total future predicted results, the climate change mostly led the future impact on the predicted results. For the future vegetation impact on hydrological components, soil moisture was more sensitive than dam inflow and evapotranspiration.

The future hydrologic conditions cannot be projected exactly due to the uncertainty in climate change scenarios and GCM outputs. However, the results of this research should be identified and incorporated into water resources planning and management in order to promote more sustainable water demand and water availability for a mountainous watershed in our country.

## Acknowledgements

This paper was supported by Konkuk University in 2012.

## References

- Ahn, S. R., Park, G. A., Jung, I. K., Lim, K. J., and Kim, S. J. (2011). "Assessing hydrologic response to climate change of a stream watershed using SLURP hydrological model." *KSCE Journal of Civil Engineering*, KSCE, Vol. 15, No. 1, pp. 43-55.
- Alcamo, J., Döll, P., Kaspar, F., and Siebert, S. (1997). *Global change and global scenarios of water use and availability: An application of water GAP 1.0. report A9701*, Center for Environmental Systems Research, University of Kassel, Germany.
- Allen, R. G. (1986). "A penman for all seasons." *Journal of Irrigation and Drain Engineering*, American Society of Civil Engineers, Vol. 112, No. 4, pp. 348-368.
- Allen, R. G., Jensen, M. E., Wright, J. L., and Burman, R. D. (1989). "Operational estimates of evapotranspiration." *Agronomy Journal*, Vol. 81, No. 4, pp. 650-662.
- Arnold, J. G. and Fohrer, N. (2005). "SWAT2000: Current capabilities and research opportunities in applied watershed modeling." *Hydrological Processes*, Vol. 19, No. 3, pp. 563-572.
- Arnold, J. G., Srinivasan, R., Mutiah, R. S., and Williams, J. R. (1998). "Large-area hydrologic modeling and assessment: Part I. Model development." *Journal of the American Water Resources Association*, Vol. 34, No. 1, pp. 73-89.
- Bärlund, I., Kirkkala, T., Malve, O., and Kämäri, J. (2007). "Assessing SWAT model performance in the evaluation of management actions for the implementation of the water framework directive in a Finnish catchment." *Environmental Modelling & Software*, Vol. 22, No. 5, pp. 719-724.
- Chaplot, V. (2007). "Water and soil resources response to rising levels of atmospheric CO<sub>2</sub> concentration and to changes in precipitation and air temperature." *Journal of Hydrology*, Vol. 337, Nos. 1-2, pp. 159-171.
- Diaz-Nieto, J. and Wilby, R. L. (2005). "A comparison of statistical downscaling and climate change factor methods: Impacts on low flows in the River Thames, United Kingdom." *Climatic Change*, Vol. 69, Nos. 2-3, pp. 245-268.
- Droogers, P. and Aerts, J. (2005). "Adaptation strategies to climate change and climate variability: A comparative study between seven contrasting river basins." *Physics and Chemistry of the Earth*, Vol. 30, Nos. 6-7, pp. 339-346.
- Eckhardt, K., Fohrer, N., and Frede, H. G. (2005). "Automatic model calibration." *Hydrological Processes*, Vol. 19, No. 3, pp. 651-658.
- Eckhardt, K., and Ulbrich, U. (2003). "Potential impacts of climate change on groundwater recharge and streamflow in a central European low mountain range." *Journal of Hydrology*, Vol. 284, Nos. 1-4, pp. 244-252.
- Fontaine, T. A., Klassen, J. F., Cruickshank, T. S., and Hotchkiss, R. H. (2001). "Hydrological response to climate change in the Black Hills of South Dakota, USA." *Hydrological Sciences Journal*, Vol. 46, No. 1, pp. 27-40.
- Gassman, P. W., Reyes, M. R., Green, C. H., and Arnold, J. G. (2007). "The soil and water assessment tool: Historical development, applications, and future research directions." *American Society of Agricultural and Biological Engineers*, Vol. 50, No. 4, pp. 1211-250.
- Gleick, P. H. and Adams, D. B. (2000). *Water: The potential consequences of climate variability and change*, The Report of the National Assessment, U.S. Global Change Research Program, U.S. Geological Survey, U.S. Department of the Interior, and the Pacific Institute for Studies in Development, Environment, and Security. Oakland, California, USA.
- Gosain, A. K., Rao, S., and Basuray, D. (2006). "Climate change impact assessment on hydrology of Indian River basins." *Current Sciences*, Vol. 90, No. 3, pp. 346-353.
- Ha, R., Shin, H. J., Park, M. J., and Kim, S. J. (2010). "Comparison of hydrological responses by two different satellite remotely sensed leaf area indices in a mountainous watershed of South Korea." *KSCE Journal of Civil Engineering*, KSCE, Vol. 14, No. 5, pp. 785-796.
- Hargreaves, G. H. and Samani, Z. A. (1985). "Reference crop evapotranspiration from temperature." *Applied Engineering in Agriculture*, Vol. 1, No. 2, pp. 96-99.
- Heuvelmans, G., Muys, B., and Feyen, J. (2006). "Regionalisation of the parameters of a hydrological model: Comparison of linear regression models with artificial neural nets." *Journal of Hydrology*, Vol. 319, Nos. 1-4, pp. 245-265.
- IPCC (1996). *Climate change 1995: Impacts, adaptation and mitigation of climate change: Scientific-technical analyses*, Contribution of Working Group II to the Second Assessment Report of the Intergovernmental Panel on Climate Change, Cambridge University Press, Cambridge, UK, New York, USA.
- IPCC (2006). *IPCC data distribution centre*, Available at: <[http://www.ipcc-data.org/sres/cgem1\\_info.html](http://www.ipcc-data.org/sres/cgem1_info.html)>
- Jensen, M. E. and Burman, R. D. (1990). *Evapotranspiration and irrigation water requirements*, ASCE Manuals and Reports on Engineering Practice No. 70, Allen, R. G. (Editors), American Society of Civil Engineers. N.Y.
- Jha, M., Arnold, J. G., Gassman, P. W., Giorgi, F., and Gu, R. (2006). "Climate change sensitivity assessment on upper Mississippi River basin streamflows using SWAT." *Journal of the American Water Resources Association*, Vol. 42, No. 4, pp. 997-1015.
- Jha, M., Pan, Z., Takle, E. S., and Gu, R. (2004). "Impacts of climate change on streamflow in the upper Mississippi River basin: A regional climate model perspective." *Journal of Geophysical Research*, Vol. 109, No. D09105, DOI:10.1029/2003JD003686.
- Monteith, J. L. (1965). "Evaporation and the environment." *The state and movement of water in living organisms*, 19th Symposia of the Society for Experimental Biology, Cambridge Univ. Press, London, U.K., pp. 205-234.
- Muleta, M. K. and Nicklow, J. W. (2005). "Sensitivity and uncertainty analysis coupled with automatic calibration for a distributed watershed model." *Journal of Hydrology*, Vol. 306, Nos. 1-4, pp. 127-145.
- Mutiah, R. S. and Wurbs, R. A. (2002). "Scaledependent soil and climate variability effects on watershed water balance of the SWAT model."

- Journal of Hydrology*, Vol. 256, Nos. 3-4, pp. 264-285.
- Nash, J. E. and Sutcliffe, J. V. (1970). "River flow forecasting through conceptual models: Part 1 - A discussion of principles." *Journal of Hydrology*, Vol. 10, No. 3, pp. 282-290.
- Park, J. Y., M. J. Park, H. K. Joh, H. J. Shin, H. J. Kwon, R. Srinivasan, and Kim, S. J. (2011). "Assessment of MIROC3.2 hires climate and CLUE-s land use change impacts on watershed hydrology using SWAT." *Trans. ASABE*, Vol. 54, No. 5, pp. 1713-1724.
- Priestley, C. H. B. and Taylor, R. J. (1972). "On the assessment of surface heat flux and evaporation using large-scale parameters." *Monthly Weather Review*, Vol. 100, No. 2, pp. 81-92.
- Rosenberg, N. J., Brown, R. A., Izaurralde, R. C., and Thomson, A. M. (2003). "Integrated assessment of Hadley Centre (HadCM2) climate change projections in agricultural productivity and irrigation water supply in the conterminous united states: I. Climate change scenarios and impacts on irrigation water supply simulated with the HUMUS model." *Agricultural and Forest Meteorology*, Vol. 117, Nos. 1-2, pp. 73-96.
- Rosenberg, N. J., Epstein, D. L., Wang, D., Vail, L., Srinivasan, R., and Arnold, J. G. (1999). "Possible impacts of global warming on the hydrology of the Ogallala aquifer region." *Climate Change*, Vol. 42, No. 4, pp. 677-692.
- Ryu, J. H., Lee, J. H., Jeong, S. M., Park, S. K., and Han, K. H. (2011). "The impacts of climate change on local hydrology and low flow frequency in the Geum River basin, Korea." *Hydrological Processes*, Vol. 25, No. 22, pp. 3437-3447.
- Stonefelt, M. D., Fontaine, T. A., and Hotchkiss, R. H. (2000). "Impacts of climate change on water yield in the upper Wind River basin." *Journal of the American Water Resources Association*, Vol. 36, No. 2, pp. 321-336.
- Takle, E. S., Jha, M., and Anderson, C. J. (2005). "Hydrological cycle in the upper Mississippi River basin: 20th century simulations by multiple GCMs." *Geophysical Research Letters*, Vol. 32, No. 18, pp. L18407.1-L18407.5.
- Thomson, A. M., Brown, R. A., Rosenberg, N. J., Izaurralde, R. C., Legler, D. M., and Srinivasan, R. (2003). "Simulated impacts of ElNino/southern oscillation on United States water resources." *Journal of the American Water Resources Association*, Vol. 39, No. 1, pp. 137-148.
- USDA Soil Conservation Service (USDA-SCS) (1972). *National engineering handbook*, Section 4 Hydrology 1972 (Chapters 4-10).
- Water Resources Update (2003). *Is global climate change research relevant to Day-to-Day water resources management*, No. 124.
- Wilby, R. L. and Harris, I. (2006) "A framework for assessing uncertainties in climate change impacts: Low flow scenarios for the River Thames, UK." *Water Resources Research*.
- Zhang, G. H. (2007). "Predicting hydrologic response to climate change in the Luohe River Basin Using the SWAT model." *Trans. of ASAE*. Vol. 50, No. 3, pp. 901-910.